

## Heat flow in the SAFOD pilot hole and implications for the strength of the San Andreas Fault

Colin F. Williams,<sup>1</sup> Frederick V. Grubb,<sup>2</sup> and S. Peter Galanis Jr.<sup>1</sup>

Received 22 December 2003; revised 12 February 2004; accepted 23 February 2004; published 24 June 2004.

[1] Detailed thermal measurements have been acquired in the 2.2-km-deep SAFOD pilot hole, located 1.8 km west of the SAF near Parkfield, California. Heat flow from the basement section of the borehole (770 to 2160 m) is 91 mW m<sup>-2</sup>, higher than the published 74 mW m<sup>-2</sup> average for the Parkfield area. Within the resolution of the measurements, heat flow is constant across faults that intersect the borehole, suggesting that fluid flow does not alter the conductive thermal regime. Reanalysis of regional heat flow reveals an increase in heat flow along the SAF northwest of Parkfield. This transition corresponds to a shallowing base of seismicity and a change in fault behavior near the northern terminus of the M6 1966 Parkfield earthquake rupture. The persistence of elevated heat flow in the Coast Ranges to the west appears to rule out frictional heating on the SAF as the source of the SAFOD value. *INDEX TERMS:* 0915

Exploration Geophysics: Downhole methods; 5134 Physical Properties of Rocks: Thermal properties; 7230 Seismology: Seismicity and seismotectonics; 8130 Tectonophysics: Heat generation and transport; 8164 Tectonophysics: Stresses—crust and lithosphere. **Citation:** Williams, C. F., F. V. Grubb, and S. P. Galanis Jr. (2004), Heat flow in the SAFOD pilot hole and implications for the strength of the San Andreas Fault, *Geophys. Res. Lett.*, 31, L15S14, doi:10.1029/2003GL019352.

### 1. Introduction

[2] The state of stress at seismogenic depths in the vicinity of the San Andreas Fault (SAF) has been the subject of intense investigation and controversy [see *Townend and Zoback*, 2004]. One approach to quantifying the average resisting stress on active faults has been to examine evidence for heat generation from frictional sliding. For Coulomb failure with dynamic and static friction coefficients consistent with laboratory measurements [e.g., *Byerlee*, 1978], the average frictional strength of the SAF should be on the order of 100 MPa. Sustained fault slip over geologic time against this frictional resistance should produce a detectable heat flow anomaly centered on the fault [*Brune et al.*, 1969; *Lachenbruch and Sass*, 1980]. In a comprehensive survey of heat flow in the vicinity of the SAF, *Lachenbruch and Sass* [1980] followed on the work of *Brune et al.* [1969] and *Heney and Wasserburg* [1971] in establishing the absence of the predicted frictional heat flow anomaly. On the basis of these results *Lachenbruch and Sass* concluded that the average static strength of the SAF does not exceed 20 MPa. Subsequent heat flow measure-

ments in the 3.5-km-deep Cajon Pass scientific drillhole confirmed the results of the shallow (typically <200 m) measurements near the Mojave segment of the SAF [*Sass et al.*, 1991], although questions remain regarding potential advective and convective disturbances to the conductive thermal regime [*Williams and Narasimhan*, 1989; *Saffer et al.*, 2003].

[3] *Sass et al.* [1997] published the results of 17 heat flow measurements along a 50-km long segment of the SAF near Parkfield, filling a large gap in the near-fault heat flow dataset. In contrast with the majority of heat flow measurements in California, the accuracy of those acquired at Parkfield was limited by sparse thermal conductivity measurements, a relatively shallow depth of investigation compared to the likely effects of surrounding topography, and possible thermal refraction due to juxtaposition of low conductivity sediments with higher conductivity Salinian and Franciscan basement rocks in the shallow subsurface [*Sass et al.*, 1997]. Although scattered, the results were consistent with a low-strength fault, with the average Parkfield heat flow of 74 mW m<sup>-2</sup> representing a transitional value between high heat flow (~85 mW m<sup>-2</sup>) in the Coast Ranges to the west and lower heat flow (<65 mW m<sup>-2</sup>) in the Great Valley to the east.

[4] The SAFOD experiment, in addition to yielding in situ information on the chemical, thermal and physical properties of the fault at depth, provides an important opportunity to compare the shallow Parkfield data with a deep profile of heat flow. The greater depth of the measurements reduces the influence of surface topography and refraction. A detailed examination of vertical variations in heat flow, particularly across faults and lithologic contacts, also provides quantitative constraints on the possible magnitude of advective heat transport.

### 2. Heat Flow in the Parkfield Area

[5] The SAFOD site is located northwest of Parkfield, approximately 1.8 km west of the SAF (Figure 1). This places it northwest of all but one of the Parkfield heat flow measurements reported by *Sass et al.* [1997] and approximately 20 km southeast of a set of five heat flow measurements in and near Pancho Rico Canyon published by *Lachenbruch and Sass* [1980]. Because the Parkfield and Pancho Rico data include heat flow values that were determined from both measured and estimated thermal conductivities and were not corrected for the thermal effects of varying topography by the same method, the combined dataset was reexamined using a single, consistent approach. Temperature gradients were corrected for local topography using the three-dimensional terrain correction method of *Birch* [1950], and heat flow values for those holes with measured thermal conductivities were distinguished from

<sup>1</sup>U.S. Geological Survey, Menlo Park, California, USA.

<sup>2</sup>U.S. Geological Survey, Sacramento, California, USA.

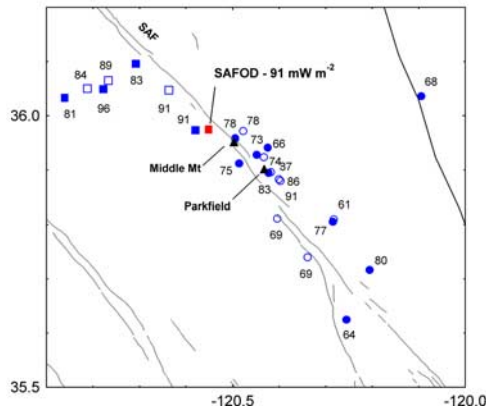


**Figure 1.** Map of Parkfield region showing heat flow measurements (circles and squares), active faults (gray) and the Coast Ranges-Great Valley (CR-GV) physiographic boundary (black). Solid symbols represent heat flow determined in holes with thermal conductivity data. Open symbols represent heat flow determined from average formation conductivities. Squares are measurements northwest of a line normal to the SAF through the SAFOD site. Circles are measurements southeast of that line.

those with conductivities estimated from formation averages. The revised values are summarized in Table 1 and shown in Figure 1.

[6] For the data published by *Sass et al.* [1997], the average of the revised values is similar (77 vs. 74  $\text{mW m}^{-2}$ ), but the range of variation has been reduced by 28 percent, from 38 to 27  $\text{mW m}^{-2}$ . Two new points, PRSN (Pearson 1-B exploratory oil well) and SFD1 (SAFOD pilot hole) have been added. The SAFOD results are discussed in full below. The value for PRSN was determined by combining the PRSN

**Table 1.** Heat Flow in the Parkfield Region

Well	Latitude	Longitude	$Q_{\text{PUB}}(\text{mW m}^{-2})^{\text{a}}$	$Q_{\text{REV}}(\text{mW m}^{-2})$
PDRH	35°37.48'	120°15.31'	68	64
PDJC	35°42.98'	120°12.28'	76	80
PDWC	35°44.33'	120°20.31'	69 <sup>b</sup>	NA
PSC2	35°48.30'	120°17.04'	69	77
PDSC	35°48.59'	120°16.92'	54	61
PDCH	35°48.66'	120°24.20'	78	69
PDHF	35°52.76'	120°23.73'	92	91
PHF2	35°52.90'	120°24.03'	84	86
EDE2	35°53.61'	120°25.32'	79	83
EADE	35°53.73'	120°24.97'	83	87
FROL	35°54.66'	120°29.10'	73	75
PDDL	35°55.37'	120°25.96'	77	74
PDL2	35°56.46'	120°25.40'	65	66
VARP	35°55.64'	120°26.81'	70	73
VARN	35°57.42'	120°29.64'	70	78
PPC2	35°58.21'	120°28.64'	82	78
SFD1	35°58.45'	120°33.06'	NA	91
PRSN	36°02.83'	120°38.20'	NA	91
PDSM	35°58.34'	120°34.72'	75	91
PR1	36°01.9'	120°51.6'	84	81
PR2	36°03.0'	120°48.7'	84	84
PR3	36°03.9'	120°46.0'	100	89
PR4	36°05.7'	120°42.5'	88	83
US1	36°02.97'	120°46.86'	94	96

<sup>a</sup> $Q_{\text{PUB}}$  are measurements published in *Lachenbruch and Sass* [1980] and *Sass et al.* [1997].  $Q_{\text{REV}}$  are new and revised measurements.

<sup>b</sup>Values in italics represent heat flow calculated using thermal conductivity values estimated from formation averages or nearby wells.

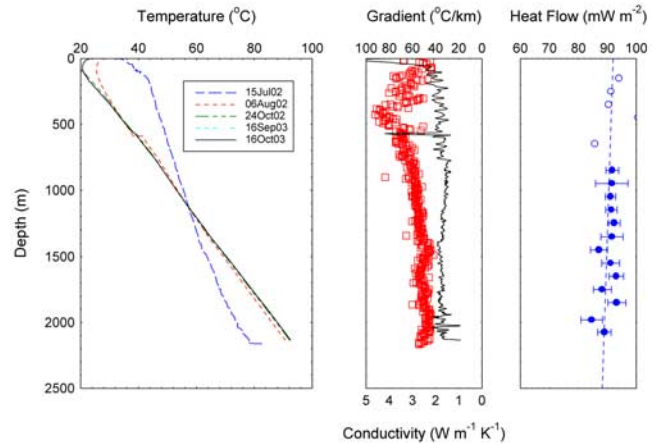


**Figure 2.** Temperature, temperature gradient, thermal conductivity (squares), and heat flow in the SAFOD pilot hole. Open circles in heat flow are estimates assuming a sediment porosity of 0.2. These estimates were not used in calculating the average SAFOD heat flow.

temperature gradient [*Sass et al.*, 1997] with sediment grain conductivity measurements from the SAFOD pilot hole over intervals that could be correlated between the two wells. Porosities for the sedimentary section in PRSN were determined from electric log density measurements and applied in the geometric mean model of *Woodside and Messmer* [1961] to determine whole rock thermal conductivities.

### 3. SAFOD Data

[7] Five temperature logs were recorded in the SAFOD pilot hole, with the first on July 13, 2002 immediately after the end of drilling and the last on October 16, 2003 (Figure 2). This 15-month period is approximately 10 times the time spent drilling the hole, and analytical models for the recovery of the hole to thermal equilibrium following the drilling disturbance [*Lachenbruch and Brewer*, 1959] indicate that the most recent log reproduces the equilibrium geothermal gradient within the resolution of the measurements. The average gradient ranges from 27 to 40°C/km, with major transitions at the sediment/basement interface (770 m) and the intersection of the hole with a major shear zone centered at approximately 1380 m [*Boness and Zoback*, 2004]. Temperature near the bottom of the hole, at 2160 m, is 93°C.

[8] Drill cuttings were collected at 6.1 m (20 ft) depth intervals for 352 thermal conductivity measurements using the chip technique of *Sass et al.* [1971]. As expected for a conduction-dominated thermal regime, the variation in thermal conductivity with depth mirrors the variation in geothermal gradient (Figure 2). The decrease in thermal conductivity and the corresponding increase in the temperature gradient below 1380 m correlates with a decrease in the quartz content of the granitic basement (M. Rymer, personal communication). Measured thermal conductivities were corrected to in situ temperatures using the correction applied by *Sass et al.* [1991] to the data from the Cajon Pass hole. The equation applied in the correction is

$$\lambda(T) = \frac{\lambda_0}{a + bT} \quad (1)$$

where  $\lambda(T)$  is the thermal conductivity at temperature  $T$ ,  $\lambda_0$  is the conductivity at  $0^\circ\text{C}$ ,  $a = 1.0$ , and  $b = 0.0024 - 0.0052/\lambda_0$ , as determined by *Williams and Sass* [1996] from measurements on representative Coast Ranges rocks at elevated temperature and pressure.

[9] Heat flow was calculated over 100 m intervals from 700 to 2200 m except at 1380 m where both the measured gradient and conductivity show significant offsets (Figure 2). Each measurement represents the product of the harmonic mean thermal conductivity and the least-squares temperature gradient over the specified depth interval. The heat flow values range from  $85$  to  $93 \text{ mW m}^{-2}$ , with a mean of  $91 \pm 3 \text{ mW m}^{-2}$  (95% confidence limits). Plotted with the heat flow measurements in Figure 2 is a predicted curve for a surface heat flow of  $93 \text{ mW m}^{-2}$  and a decrease in heat flow with depth of  $1.4 \text{ mW m}^{-2}$  per km due to the contribution of radiogenic heat production as estimated from SAFOD electric log natural gamma data using the relation of *Rybach* [1986]. This predicted decrease with depth yields the average value measured in the basement section.

[10] Within the resolution of the measurements, heat flow in the SAFOD pilot hole does not vary beyond the modest decline due to the decreasing contribution of radiogenic heat production with depth, and even that predicted decline cannot be differentiated from constant heat flow with depth. Heat flow is constant across the fault zones and fractured intervals that intersect the borehole at 1150–1220, 1345–1420 and 1820–1880 m [*Boness and Zoback*, 2004]. This result is consistent with the view that heat transport in the upper crust along this segment of the SAF is by conduction and is not influenced by ground-water flow. One-dimensional models for the combined thermal effects at the SAFOD site of uplift and erosion over the past 10 Ma along with earlier Tertiary sedimentation indicate that the resulting disturbance to measured heat flow is less than 5% [*Blythe et al.*, 2004; *Lachenbruch et al.*, 1995].

#### 4. Analysis

[11] The predominant feature of the new and revised heat flow measurements is the contrast in heat flow along the SAF northwest and southeast of Middle Mt. (Figure 1). Mean heat flow for the five sites northwest of Middle Mt. with values determined from temperatures and thermal conductivities measured in the same borehole is  $88.5 \pm 5.6 \text{ mW m}^{-2}$ , compared to a mean of  $74.5 \pm 4.7 \text{ mW m}^{-2}$  for the equivalent eight sites southeast of Middle Mt. Only one of these eight measurements southeast of Middle Mt. (EDE2 –  $83 \text{ mW m}^{-2}$ ) exceeds the lowest value among the five to the northwest (PR1 –  $81 \text{ mW m}^{-2}$ ).

[12] This increase in heat flow along-strike correlates with other characteristics of the SAF near Parkfield. The hypocenter of the 1966 M6 Parkfield earthquake was located under Middle Mt., with coseismic slip focused exclusively to the southeast. As first defined through geodetic modeling by *Harris and Segall* [1987] and confirmed through refined analysis of GPS data by *Murray et al.* [2001], the section of the fault ruptured by the 1966 earthquake currently forms a locked patch, with fault slip at rates greater than 5 mm/yr occurring only in the upper 2 to 3 km of the fault and below the seismogenic zone at approximately 14 km. The locked patch as defined by *Murray et al.* [2001] is eroded to the northwest along strike

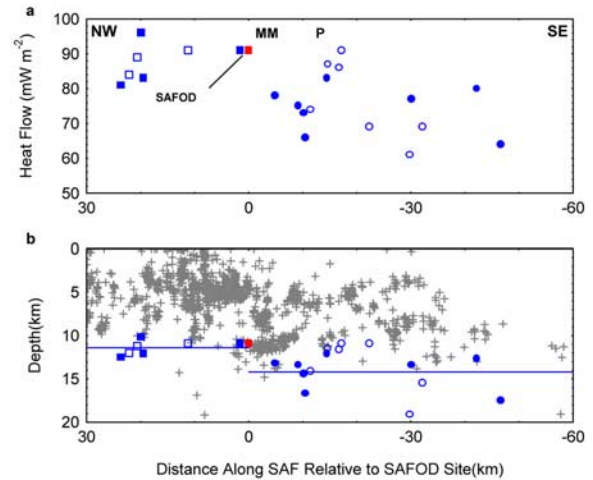


**Figure 3.** (a) Section along-strike of the SAF showing heat flow from Figure 1. (b)  $M > 1.5$  Calnet seismicity for the period 1980–2003 (crosses), estimated depths to  $350^\circ\text{C}$  isotherm from heat flow, and average isotherm depths northwest and southeast of SAFOD (blue lines). Middle Mt. (MM) and Parkfield (P) are indicated.

with increasing slip rate from both above and below through a transition to the creeping segment of the SAF. Along the creeping section fault slip exceeds 25 mm/yr through the entire seismogenic zone. According to *Eberhart-Phillips and Michael* [1993], the onset of fault creep corresponds with a region of low crustal seismic velocities in the Franciscan terrain northeast of Middle Mt. which may reflect elevated pore fluid pressure in the rocks bounding the SAF along the creeping segment.

[13] The lower boundary of the seismogenic zone also shallows along this segment of the fault. The depth above which 95% of the earthquakes occur averages approximately 13 km southeast of the SAFOD site and approximately 10 km northwest of the SAFOD site (Figure 3). This relative depth variation is confirmed in seismicity near Middle Mt. relocated by the double-difference technique (W. Ellsworth, personal communication). To examine the relationship between the shallowing base of seismicity and deep thermal conditions, geotherms were calculated for each of the measurements in Table 1. According to *Williams* [1996], for conductive heat flow in a crustal layer of constant heat production  $A$ , surface heat flow  $q_s$ , and thermal conductivity given by equation (1), temperature varies with depth  $z$  according to

$$T(z) = \frac{1}{b} \cdot [\exp(c_1 z - c_2 z^2 + c_3) - a] \quad (2)$$

where  $c_1 = bq_s/\lambda_0$ ,  $c_2 = bA_s/2\lambda_0$ , and  $c_3 = \ln(a + bT)$ . The calculated depth to the  $350^\circ\text{C}$  isotherm for each heat flow measurement is plotted in Figure 3. Both the  $350^\circ\text{C}$  isotherms and the base of seismicity shallow from southeast to northwest by approximately 3 km. The average depth of the  $350^\circ\text{C}$  isotherm northwest of Middle Mt. is 11.0 km and southeast of Middle Mt. is 14.2 km.

[14] Although spatially correlated, the relationship between active fault slip and elevated heat flow is not straightforward. Fault slip along the creeping section is a

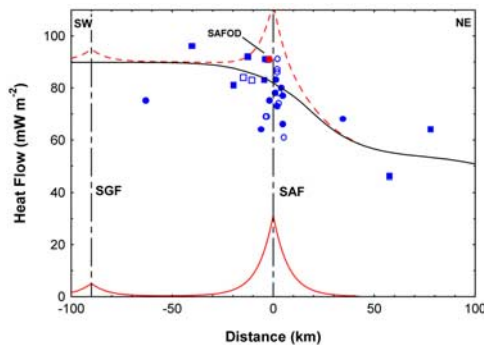


**Figure 4.** Southwest-northeast section normal to the SAF showing the SAF and San Gregorio-Hosgri fault (SGF), heat flow, the predicted frictional heat-flow anomaly (solid red), the modeled CR-GV heat flow transition (solid black), and the superposition of the anomaly on the model (dashed red).

consequence of conditional frictional stability possibly related to elevated pore pressure [Scholz, 1998]. Consequently it is not thermally activated, but higher temperatures can weaken the fault at depth. The base of the seismogenic zone reflects a frictional stability transition from stick-slip to stable sliding, and there is evidence that this stability transition may correspond to the onset of plastic flow for constituent minerals in the fault zone [e.g., Scholz, 1998]. The transition from brittle failure to plastic flow is controlled by ambient thermal conditions, and higher heat flow along the SAF northwest of Parkfield may facilitate creep by reducing the depth of stable sliding and by lowering both the peak and average brittle strength of the fault.

[15] Recognition of the systematic along-strike variation in heat flow reduces the uncertainty associated with estimating the possible level of frictional heating along this segment of the SAF. Figure 4 shows heat flow projected on a plane normal to the fault zone, with measurements northwest of SAFOD differentiated from those southeast of SAFOD. Also shown is the expected frictional heat flow anomaly for the SAF and San Gregorio-Hosgri fault as well as a model heat flow profile for the thermal transition from the Coast Ranges to the Great Valley [Williams *et al.*, 2000]. Although there remains significant scatter among the measurements southeast of SAFOD, neither dataset shows any indication of elevated heat flow along the SAF compared to far-field values, confirming the original observations of Lachenbruch and Sass [1980] and Sass *et al.* [1997].

## 5. Summary

[16] Heat flow measurements from 770 to 2200 m depth in the SAFOD pilot hole average  $91 \pm 3 \text{ mW m}^{-2}$ , and there are no resolvable thermal perturbations due to advective transport of heat along the faults and fracture zones that intersect the borehole. The SAFOD heat flow value is consistent with a transition in heat flow along the SAF from an average of  $77 \text{ mW m}^{-2}$  in the region southeast of Middle Mt. to an average of  $88 \text{ mW m}^{-2}$  to the northwest. This thermal transition correlates with a shallowing of the base of recorded seismicity and with the southeastern boundary of the creeping section of the SAF. Thermal weakening of the SAF at depth and the corresponding thinning of the portion

of the fault characterized by brittle failure may facilitate the extension of fault creep from the surface down through the entire seismogenic zone. Analysis of the new heat flow measurements with revised published values confirms the absence of a fault-centered frictional heat flow anomaly.

## References

- Birch, F. (1950), Flow of heat in the Front Range, Colorado, *Geol. Soc. Am. Bull.*, *61*, 567–630.
- Blythe, A. E., M. A. d'Alessio, and R. Bürgmann (2004), Constraining the exhumation and burial history of the SAFOD pilot hole with apatite fission track and (U-Th)/He thermochronometry, *Geophys. Res. Lett.*, *31*, L15S16, doi:10.1029/2003GL019407.
- Boness, N. L., and M. D. Zoback (2004), Stress-induced seismic velocity anisotropy and physical properties in the SAFOD Pilot Hole in Parkfield, CA, *Geophys. Res. Lett.*, *31*, L15S17, doi:10.1029/2003GL019020.
- Brune, J. N., T. L. Heney, and R. F. Roy (1969), Heat flow, stress, and rate of slip along the San Andreas Fault, California, *J. Geophys. Res.*, *74*, 3821–3827.
- Byerlee, J. D. (1978), Friction of rock, *Pure Appl. Geophys.*, *116*, 615–626.
- Eberhart-Phillips, D., and A. J. Michael (1993), Three-dimensional velocity structure, seismicity, and fault structure in the Parkfield region, central California, *J. Geophys. Res.*, *98*, 15,737–15,758.
- Harris, R. A., and P. Segall (1987), Detection of a locked zone at depth on the Parkfield, California, segment of the San Andreas Fault, *J. Geophys. Res.*, *92*, 7945–7962.
- Heney, T. L., and G. J. Wasserburg (1971), Heat flow near major strike-slip faults in California, *J. Geophys. Res.*, *76*, 7924–7946.
- Lachenbruch, A. H., and M. C. Brewer (1959), Dissipation of the temperature effect of drilling a well in Arctic Alaska, *U.S. Geol. Surv. Bull.*, *1083-C*, 73–109.
- Lachenbruch, A. H., and J. H. Sass (1980), Heat flow and energetics of the San Andreas fault zone, *J. Geophys. Res.*, *85*, 6185–6223.
- Lachenbruch, A. H., J. H. Sass, G. D. Clow, and R. Weldon (1995), Heat flow at Cajon Pass, California, revisited, *J. Geophys. Res.*, *100*, 2005–2012.
- Murray, J. R., P. Segall, P. Cervelli, W. Prescott, and J. Svarc (2001), Inversion of GPS data for spatially variable slip-rate on the San Andreas Fault near Parkfield, CA, *Geophys. Res. Lett.*, *28*, 359–362.
- Rybach, L. (1986), Amount and significance of radioactive heat sources in sediments, in *Thermal Modeling in Sedimentary Basins*, edited by J. Burrus, pp. 311–322, Ed. Tech., Paris.
- Saffer, D. M., B. A. Bekins, and S. Hickman (2003), Topographically driven groundwater flow and the San Andreas heat flow paradox revisited, *J. Geophys. Res.*, *108*(B5), 2274, doi:10.1029/2002JB001849.
- Sass, J. H., A. H. Lachenbruch, and R. J. Munroe (1971), Thermal conductivity of rocks from measurements on fragments and its application to heat-flow determinations, *J. Geophys. Res.*, *76*, 3391–3401.
- Sass, J. H., A. H. Lachenbruch, T. H. Moses Jr., and P. Morgan (1991), Heat flow from a scientific research well at Cajon Pass, California, *J. Geophys. Res.*, *97*, 5017–5030.
- Sass, J. H., C. F. Williams, A. H. Lachenbruch, S. P. Galanis Jr., and F. V. Grubb (1997), Thermal regime of the San Andreas Fault near Parkfield, California, *J. Geophys. Res.*, *102*, 27,575–27,585.
- Scholz, C. H. (1998), Earthquakes and friction laws, *Nature*, *391*, 37–42.
- Townend, J., and M. D. Zoback (2004), Regional tectonic stress near the San Andreas Fault in central and southern California, *Geophys. Res. Lett.*, *31*, L15S11, doi:10.1029/2003GL018918.
- Williams, C. F. (1996), Temperature and the seismic/aseismic transition: Observations from the 1992 Landers earthquake, *Geophys. Res. Lett.*, *23*, 2029–2032.
- Williams, C. F., and T. N. Narasimhan (1989), Hydrogeologic constraints on heat flow along the San Andreas Fault: A testing of hypotheses, *Earth Planet. Sci. Lett.*, *92*, 131–143.
- Williams, C. F., and J. H. Sass (1996), The thermal conductivity of rock under hydrothermal conditions—Measurements and applications, paper presented at 21st Annual Workshop: Geothermal Reservoir Engineering, Stanford Geotherm. Program, Stanford, Calif.
- Williams, C. F., A. H. Lachenbruch, and J. H. Sass (2000), Heat flow and the San Andreas Fault, *Eos. Trans. AGU*, *81*(48), Fall Meet. Suppl., T11E-08.
- Woodside, W., and J. Messmer (1961), Thermal conductivity of porous media, *J. Appl. Phys.*, *32*, 1688–1706.

S. P. Galanis Jr. and C. F. Williams, U.S. Geological Survey, 345 Middlefield Road, Menlo Park, CA 94025, USA. (colin@usgs.gov)

F. V. Grubb, U.S. Geological Survey, Placer Hall, Sacramento, CA 95819, USA.